frontiers | Frontiers in Environmental Science

ORIGINAL RESEARCH
published: 26 May 2022
doi: 10.3389/fenvs.2022.908984

Modeling Emulsification Influence on Oil Properties and Fate to Inform Effective Spill Response

Deborah P. French-McCay, Matthew Frediani and Melissa D. Gloekler*

RPS Oceans and Coastal, South Kingstown, RI, United States

Water-in-oil emulsification affects spilled oil fate and exposure, as well as the effectiveness of oil spill response options, *via* changes in oil viscosity. While oil weathering processes such as evaporation, dissolution, photo-oxidation, and biodegradation increase oil viscosity about 10-fold, incorporation of water droplets into floating oil can increase viscosity by another order of magnitude. The objective of this study was to evaluate how changes in viscosity by oil type, with weathering, and with emulsification affect oil fate. Oil spill modeling analyses demonstrated that the increase in viscosity from emulsification prolonged floating oil exposure by preventing the oil from dispersing into the water column. Persistent emulsified oils are more likely to come ashore than low viscosity oils that readily disperse. Through a rapid increase in viscosity, emulsification restricted entrainment and slowed evaporation. Water column exposure to dissolved concentrations increased with lower viscosity oils. Thus, the ability to emulsify, and at what weathered state, are important predictors of oil fate. Oil viscosity is an important consideration for choosing response alternatives as it controls effectiveness of mechanical removal, *in-situ*-burning and surface-active chemicals. Therefore, understanding and quantification of oil emulsification are research priorities. The most influential model input determining emulsification and the emulsion's viscosity is its maximum water content, as it controls the ultimate viscosity of the emulsion. Viscosities were also influenced by the volatile content and initial viscosity of the oil. Algorithms quantifying emulsion stability under field conditions have not been developed, so emulsions were assumed stable over the 30-day simulations. Changes in emulsion stability over time would affect oil properties and so floating oil and shoreline exposures, as well as response effectiveness. However, water column exposures to dissolved concentrations are determined within a few days of oil release, and as such would not be affected by differences in long-term stabilities of the emulsions.

Keywords: oil spill modeling, oil fate, water-in-oil emulsification, oil exposure, oil weathering, oil spill response, oil viscosity, oil fate and effects

OPEN ACCESS

Edited by:
Kenneth Lee,
Department of Fisheries and Oceans, Canada

Reviewed by:
Scott Pegau,
Oil Spill Recovery Institute, United States
Suneel V.,
Council of Scientific and Industrial Research (CSIR), India

****Correspondence:***
Deborah P. French-McCay
Debbie.McCay@rpsgroup.com

Specialty section:
This article was submitted to Toxicology, Pollution and the Environment, a section of the journal Frontiers in Environmental Science

Received: *31 March 2022*
Accepted: *29 April 2022*
Published: *26 May 2022*

Citation:
French-McCay DP, Frediani M and Gloekler MD (2022) Modeling Emulsification Influence on Oil Properties and Fate to Inform Effective Spill Response. Front. Environ. Sci. 10:908984. doi: 10.3389/fenvs.2022.908984

1 INTRODUCTION

When oil is spilled into water, it is subjected to various weathering processes (e.g., evaporation, dissolution, photo-oxidation) which have the potential to change the physical and chemical properties (Payne and McNabb, 1984) as well as the fate and transport of the spilled product. Depending on the *in-situ* turbulence level, the physical properties, and the chemical composition of the oil, and the various weathering processes the oil is subjected to while at sea, some oils form water-

in-oil emulsions. Water-in oil emulsions (also referred to as mousse) may contain as much as 80% water in the form of micrometer-sized droplets dispersed within a continuous phase of oil (Daling and Brandvik 1988; Fingas et al., 1995; Fingas et al., 1997).

The formation of water-in-oil emulsions (herein referred to as emulsions) from spilled oil affects cleanup operations and potentially reduces response options (e.g., efficacy of mechanical recovery) or the window of opportunity for such operations (e.g., dispersant use; National Academies of Sciences, Engineering, and Medicine (NASEM), 2020). Emulsion formation depends on the oil's bulk properties (e.g., viscosity and density) and composition (e.g., asphaltene, resin, and wax content) combined with environmental factors, such as light exposure and local ocean turbulence level. The viscosity of an emulsified oil tends to be much higher than a fresh oil or oil that experienced evaporative weathering alone (Daling and Brandvik, 1988; Fingas et al., 1995; Fingas et al., 1997; Daling et al., 2014). As a result of emulsification, an increase in the oil's viscosity reduces natural and dispersant-facilitated entrainment rates from surface water to the water column. Entrainment affects weathering processes, reducing evaporation while facilitating dissolution and biodegradation. The oil droplet size distribution (DSD) of entrained oil influences the residence time in the water column as larger droplets are more buoyant and resurface faster than smaller droplets. Thus, oil viscosity, as it changes with weathering and emulsification, is a key parameter controlling oil fate.

During emulsification, water content increases over hours to a few days (Mackay and Zagorski, 1982; Lehr, 2017) and plateaus at a maximum water content which is inversely related to the viscosity of the oil (Daling and Brandvik, 1988). For example, highly viscous oils are less likely to emulsify due to the inability for water to penetrate the continuous phase of the oil (Fingas et al., 1995). The formation of water-in-oil emulsions and their stability depend on oil bulk properties, oil composition, light exposure, and turbulence level. For many light crude oils, emulsification begins after some period of weathering, due to the concentration of asphaltenes and resins as volatile and soluble fractions evaporate or dissolve, as well as to photo-oxidation changing composition (Ward et al., 2018). The stability of emulsions has been studied in laboratory experiments, showing for some oils a loss of water content over weeks or months under quiescent conditions, but is not well understood for field conditions. The effect of photo-oxidation on emulsification is not examined here as it has not been quantified in laboratory or field studies to date. However, it has been identified as a research need. Photo-oxidation appears to enable an oil to emulsify and to stabilize emulsions.

The objective of this study was to investigate, *via* modeling, the formation of water-in-oil emulsions, as a function of oil bulk properties, oil composition, and turbulence level (environmental conditions). The implications of emulsification on response effectiveness, *via* changes in oil viscosity, and environmental exposures (to surface oil, shoreline oiling, and water column concentrations) are examined. The results demonstrate the importance of considering the emulsification process for planning and implementing response actions, as well as when evaluating potential environmental effects.

2 METHODS

This modeling sensitivity study was performed to evaluate how emulsification and resulting changes in viscosity affect oil fate for a variety of oils under a range of environmental conditions. The modeling was performed in three phases:

1) Viscosity changes with weathering and water content: The sensitivity of oil viscosity to initial (i.e., fresh) oil viscosity, evaporation, and water uptake with emulsion formation was examined. These processes are driven by oil type (and so initial viscosity and composition), temperature, wind speed, and maximum water content. To demonstrate the sensitivities of input parameters and conditions on emulsion viscosity, a matrix of predicted emulsion viscosities for various oils and weathering states was evaluated. From the results, three contrasting oils (e.g., light, medium, and heavy) were selected for further study in phases two and three.
2) Probabilistic approach: The range and variability of oil fate for potential environmental conditions (i.e., effect of winds and temperature) were evaluated using oil transport and fate modeling. Six stochastic simulations were examined, each of which included an ensemble of model simulations using the same input parameters (e.g., volume released and oil type) with start dates varied over a long-term observational wind and associated temperature record to evaluate the potential effect of environmental conditions on oil fate.
3) Deterministic analysis: Two (e.g., 95th percentile for surface oil exposure and 95th percentile for water column exposure) model runs from each of the six stochastic scenarios were examined in further detail to investigate the effect of emulsification on oil weathering and fate.

2.1 Phase 1: Oil Viscosity and Water Content Sensitivity Assessment

Thirteen well-characterized crude oils and intermediate-heavy fuel oils (**Table 1**; **Supplementary Appendix Tables A1, A2**) were selected to represent a range of oil densities. Their emulsion viscosities were calculated for different weathering states and maximum water contents using the model algorithms in the Spill Impact Model Application Package (SIMAP; French-McCay, 2003; French-McCay, 2004; French-McCay et al., 2018a; French-McCay et al., 2021a; French-McCay et al., 2021b), the oil fate model employed in this study.

2.1.1 Viscosity Change of Oil

The change in dynamic viscosity of spilled oil is estimated in the SIMAP model by combining the effects of temperature, the loss of volatiles, and water uptake by emulsification (French-McCay et al., 2018a; French-McCay et al., 2021a; French-McCay et al., 2021b).

$$\mu_t = \mu_{temp} * exp\left(C'_{evap} F_v / F_{bp380}\right) * exp\left(\frac{2.5 F_w}{1 - F_{wmax} F_w}\right)$$

where μ_t is oil dynamic viscosity (cP) at time t and ambient temperature; μ_{temp} is initial oil dynamic viscosity (cP) at ambient

TABLE 1 | Initial properties of oils used for emulsification modeling.

Oil name	API (°)	Dynamic viscosity (cP) at 25°C	Maximum percent water	Fraction volatiles (Boiling points < 380°C)	Asphaltenes (%)	Resins (%)
HFO-11-380_Prestige	10.8	8,956.9	60.0	0.16	12.4	12.0
HFO-15-IFO180	14.9	839.5	69.0	0.32	10.0	11.0
Crude-16-PlatformElly	15.8	1,408.1	64.0	0.37	13.6	19.4
Crude-20-Maya_2004	20.4	279.4	64.0	0.47	15.5	12.7
Crude-22-WCS2017	21.7	178.2	60.0	0.22	4.4	10.4
Crude-27-BowRiverBlend	27.0	22.4	66.0	0.47	8.0	4.0
Crude-31-PetroniusBlockVK786A	31.0	2.3	78.3	0.49	1.6	5.5
Crude-33-AlaskanNorthSlope2017	32.5	7.2	31.0	0.46	1.6	4.7
Crude-34-HOOPS	34.2	7.4	64.0	0.57	1.2	6.8
Crude-35-MC252_2020	35.4	4.8	64.0	0.62	0.3	10.1
Crude-37-WestTexasIntermediate	36.6	4.4	64.0	0.65	1.0	6.0
Crude-41-Bakken	40.6	3.0	0.0	0.73	0.0	10.1
Cond-49-Oso Condensate	49.2	1.5	0.0	0.82	1.2	6.8

temperature; C'_{evap} is an empirical constant (4.6077, French-McCay et al., 2018a); F_v is fraction of initially released oil mass lost to evaporation, dissolution or degradation; F_{bp380} is fraction of oil that distills below 380°C (i.e., the volatile fraction of the fresh oil); F_w is fraction of water in oil; F_{wmax} is the maximum fraction of water in fully emulsified oil. The SIMAP model calculates F_v and F_w over time, which are then used to calculate viscosity (μ_t) at time, t. In the above equation, the first term accounts for the temperature effect, the second term accounts for weathering losses of volatiles, and the third term accounts for the influence of water content on viscosity. The pertinent algorithms for the first and third terms are described below.

2.1.2 Temperature Effect on Viscosity

SIMAP uses the algorithm of Mackay et al. (1982), an Arrhenius equation, to estimate the change in viscosity (μ_{temp}, cP) due to temperature (T, in degrees K):

$$\mu_{temp} = \mu_o exp\left[C_{temp}\left(\frac{1}{T} - \frac{1}{T_o}\right)\right]$$

where μ_o is the viscosity (cP) of the fresh oil at a reference temperature T_o (K) and C_{temp} is a temperature correction factor, which is a constant for each oil type. The value of C_{temp} is estimated for each oil based on measurement data of viscosity at two different temperatures. The oil temperature, T, is not usually available so the model approximates it as the temperature of the surrounding water.

2.1.3 Modeling Emulsification

For emulsifying oils, the Mackay and Zagorski (1982) emulsification scheme is implemented (i.e., water content increases exponentially with the rate related to the square of wind speed and previous water incorporation). The change in viscosity is a function of water content.

The four states of water-in-oil emulsion classification approach defined in Fingas and Fieldhouse (2005); Fingas and Fieldhouse (2012); Fingas and Fieldhouse (2014) is employed to determine whether an oil will emulsify and to characterize emulsion stability. Based on the oil properties density, viscosity, and resin and asphaltene content at the current state of weathering and on a complex formula (see Fingas and Fieldhouse, 2012; Fingas and Fieldhouse, 2014), oils are classified as forming stable, meso-stable, entrained, or unstable water-in-oil emulsions. The SIMAP model tracks the concentrations of asphaltenes and resins, along with changes in density and viscosity, as volatile and soluble components are lost through evaporation, dissolution, and biodegradation. If the classification indicates an unstable emulsion, the oil will not emulsify, whereas water uptake is calculated for the other three classes. As the oil properties and concentrations of asphaltenes and resins in the oil change due to weathering, the oil can potentially move from one emulsification class to another. For example, if an oil is initially classified as forming an unstable emulsion, water uptake is delayed until the oil has sufficiently weathered so that the emulsion classification changes from unstable to meso-stable, stable, or entrained. Once the classification changes, water uptake is initiated, and changes in oil viscosity due to emulsification begin.

The rate at which water is incorporated into oil, dF_w/dt (s^{-1}), is given by

$$\frac{dF_w}{dt} = C_1 U_w^2 (1 - F_w/F_{wmax})$$

where C_1 is empirical constant (2×10^{-6} for emulsifying oils, i.e., meso-stable, stable, and entrained; 0 for non-emulsifying oils and unstable emulsions), U_w is wind speed (m/s), F_w is fraction of water in oil, and F_{wmax} is the maximum fraction of water in fully emulsified oil [a model input based on measurement data; typically about 0.7 for crude oils (Reed, 1989) and much lower or 0 for highly viscous oils]. As this equation does not allow for a decrease in water content, the underlying assumption is that the emulsion remains stable for the remaining duration of the model simulation. The viscosity of the emulsified oil, $\mu_{watercontent}$ (cP), is given (Mooney, 1951; Mackay et al., 1980a; Mackay et al., 1980b) as

$$\mu_{watercontent} = \mu_{temp} exp\left(\frac{2.5F_w}{1 - F_{wmax}F_w}\right)$$

where μ_{temp} is initial oil viscosity (cP) at ambient temperature, F_w is fraction of water in oil, and F_{wmax} is maximum fraction of water in oil (same as F_{wmax} in the water uptake equation above).

2.2 Phase 2: Probabilistic Oil Spill Modeling

Oil spills into offshore waters can result in trajectories that move in various directions, depending upon the winds and currents prevailing at the time. The fate of the oil is subject to the time sequence of environmental conditions at the time of and following the spill. Thus, the SIMAP oil trajectory and fate model was run in probabilistic (or "stochastic") mode, randomly varying the start date across a long-term wind data set, allowing quantification of the effect of emulsification on oil fate while considering the effect of winds that might occur during and following a spill. This provides a statistical analysis of results generated from many different individual model simulations of the same type of spill scenario. A long wind record from a meteorological buoy in the Gulf of Mexico (i.e., Station 42001, LLNR 1465—MID GULF—180 nm South of Southwest Pass, LA) was used, along with HYCOM (Chassignet and Srinivasan, 2015) hindcasted currents for the same latitude/longitude position as the meteorological buoy.

To focus results on oil fate (as opposed to trajectories), the spill site was in an open-water offshore area, distant from land. The modeling matrix involved six scenarios:

- Three crudes (West Texas Intermediate, Bow River Blend, Western Canadian Select)
- Two maximum water contents (0%, percentage appropriate to the oil type)

The stochastic analysis provided: 1) areas associated with probability of oiling; 2) the shortest time required for oil to reach any point within the areas predicted to be oiled; 3) properties (e.g., viscosity and density) and composition of oil over time as it weathered under different environmental conditions; and 4) percentages of the spilled oil in different environmental compartments over time subject to winds and other influential factors. The predicted cumulative footprints, or areas and probabilities of oiling, were generated by a statistical analysis of all the individual trajectories. The analysis evaluated areas affected and concentrations over a prescribed minimum threshold, and at oiling probabilities above a certain percent (e.g., >1%). Stochastic modeling results include predicted spatial distributions of hydrocarbons and probabilities that water surface, water column, and shoreline areas would be affected, as well as oil exposure levels. These exposures were quantified using indices of interest (e.g., water surface swept by oil, water volume contaminated). The results were summarized as mean, standard deviation, frequency distributions, and 95th percentile for variables of interest for response planning and potential impact evaluations:

- Surface area swept (km^2) by floating oil/emulsion over concentration thresholds of interest (e.g., sheen at 0.1 g/m^2 and thick oil at 10 g/m^2), based on analyses in French-McCay (2016) and French-McCay et al. (2018c);
- Sum of surface area swept (km^2) by floating oil/emulsion over the concentration threshold of interest in each time step multiplied by exposure time (i.e., the time step duration of 0.25 h), yielding an exposure index in area-time units (km^2-days);
- Maximum volume of water exposed at any time to dissolved concentrations above threshold concentrations of concern;
- Average exposure (μg/L-hours) in the volume of water affected by dissolved concentrations above threshold concentrations of concern, calculated by summing over the entire simulation volume exposed multiplied by the time step duration;
- Maximum floating oil percentage (by mass) at any time in the simulation;
- Evaporated mass percentage by the end of the simulation;
- Water column mass percentage (maximum entrained whole oil, dissolved, and total) at any time in the simulation;
- Biodegraded mass percentage by the end of the simulation; and
- Surface oil water content, viscosity, and density when fully weathered.

2.2.1 Thresholds of Concern

The model results were summarized as areas and volumes of water where oil exposure exceeded specified thresholds of concern. Thresholds of concern were reviewed by French-McCay (2016) and French-McCay et al. (2018c), based in part on work described in French-McCay (2002); French-McCay (2003); French-McCay (2004). The following thresholds, based on these reviews, were selected for this modeling study.

Floating surface oil concentration thresholds: ≥0.1 g/m^2 and ≥10 g/m^2. Oil sheens are generally 0.1–1 g/m^2 (Bonn Agreement, 2009; Bonn Agreement, 2011; National Oceanic and Atmospheric Administration (NOAA), 2016) as a spatial average over the grid cell dimensions used to represent the concentrations of floating oil. (Note that oil is patchy at small scales.) Effects on socioeconomic resources may occur (e.g., fishing may be prohibited) if oil is visible on the water surface (i.e., ≥0.1 g/m^2). Effects on wildlife (birds, mammals, and reptiles) may occur if oil on the water surface is ≥10 g/m^2. For surface oil exposure, 1 g/m^2 corresponds to approximately 1-micron thick oil, on average.

Water concentration threshold: ≥1 μg/L and 10 μg/L total dissolved polycyclic aromatic compounds, PACs. Effects on sensitive early life history stages of fish and invertebrates may occur at concentrations above approximately 1 μg/L (1 ppb) of dissolved aromatics (i.e., PACs, which include polycyclic aromatic hydrocarbons and related compounds) that make up most of the exposure concentrations. The threshold for species of typical sensitivity is about 10 μg/L (10 ppb) of dissolved PAC. Older animals are typically not affected by dissolved PAC concentrations below 100 ppb. (See French-McCay, 2002; French-McCay, 2016; French-McCay et al., 2018c for further background on these thresholds).

2.2.2 Model Inputs

Environmental data and oil property inputs are described in **Supplementary Appendix Section A**. Five years of current (**Supplementary Appendix Section A.1.1**) and wind (**Supplementary Appendix Section A.1.2**) data were sampled for running the stochastic scenarios. Gaps in the available wind record (2005–2010) dictated the choice of years. Two model runs were performed for each month during the 4 years with complete wind records (2005, 2007, 2008, and 2009), and for 9 months in 2010, selecting the start date at the beginning of each sampled half-month period. Thus, 114 runs were performed for each stochastic scenario, and each simulation was modeled for a total of 30 days. Wind roses for the data used from 2010 were very similar to the wind rose for 2005, 2007, 2008, and 2009, indicating the missing data from 2010 did not cause a bias.

The location of the meteorological buoy 42001 (25.942°N 89.657°W) was used as the spill site. Wind drift of floating oil was assumed to be typical of offshore in the northern hemisphere (i.e., the surface oil wind drift factor was 3.5% and the angle was 20° to the right of downwind). Total suspended sediment concentrations were assumed to be a typical concentration for the Gulf of Mexico, 3 mg/L (French-McCay et al., 2018a; French-McCay et al., 2018b).

Instantaneous surface releases of 200 metric tonnes (MT, ~1,250 bbls; volume varies slightly by oil type) were modeled using 15-min time steps and simulating oil fate over 30 days. Note that while concentrations and areas/volumes affected would vary by spilled amount, the weathering behavior and mass balance on a percentage basis will be representative of a range of spill sizes. The numbers of Lagrangian Elements (LEs) simulated were 2,000 surface or entrained whole oil LEs and 20,000 dissolved components LEs. Each LE representing subsurface entrained oil or dissolved components was treated as a Gaussian shaped cloud of mass, with spreading rate controlled by diffusion coefficients of 1 m^2/s in the horizontal and 10 cm^2/s in the vertical. The LE centers were dispersed by random walk-based diffusion; 10 m^2/s for floating oil, 1 m^2/s for subsurface LEs in the horizontal dimension and 10 cm^2/s for subsurface LEs in the vertical dimension.

2.2.3 Statistical Analysis

The same set of spill dates were simulated for each oil with and without inclusion of emulsification. Thus, Student's paired *t*-tests, with a two-tailed distribution, were conducted to identify significant changes between simulation results with versus without inclusion of emulsification for the same spill date. The *t*-test measures the probability that the results are not different. Probabilities <0.05 (i.e., <5%) indicate that emulsification significantly affected the results (with 95% confidence). The degrees of freedom for all these tests are equal to n/2-1, where n = 114 model runs per scenario, and df = 56.

2.3 Phase 3: Deterministic Oil Spill Model Analysis

Twelve individual ("deterministic") model simulations, four per oil, were selected from the stochastic parent scenarios to evaluate oil fate and weathering in detail. For each of the emulsified states, weathered-only (i.e., F_{wmax} = 0) and weathered and emulsified oils, the two simulations selected per stochastic scenario were: 1) 95th percentile for surface oil exposure, and 2) the 95th percentile for water column exposure. In addition to a specific trajectory, the results of the deterministic simulations provide a time history of oil weathering (as indicated by surface oil water content, viscosity, and oil density) and the oil mass balance, expressed as the percentage of spilled oil on the water surface, on the shoreline, evaporated, entrained in the water column, and degraded. The reported deterministic results include:

- Mass balance over time (expressed as % by mass of the release); and
- Maps of maximum surface oil exposure and vertical maximum water column entrained and dissolved concentrations for each deterministic run.

3 RESULTS

3.1 Phase 1: Oil Viscosity Change With Weathering and Water Content

Using the model equations (**Section 2.1**), viscosity changes with temperature, fraction weathered (F_v) and water content (F_w) calculated for the thirteen evaluated oils (**Table 1**; **Supplementary Appendix Section A.1.5**) demonstrate the functional relationships. This initial analysis showed that because the water uptake rate is related to the square of wind speed, water uptake to the maximum water content occurs within a few hours (in moderate winds 5–10 m/s) to a few days (in light winds <5 m/s) under most conditions. The modeled viscosity (assuming no emulsification) increases with loss of volatiles, primarily due to evaporation, with some losses attributed to dissolution and biodegradation (**Figure 1**). The rate of change (i.e., the slope) of viscosity with percent evaporated is constant on a log-linear scale, with the intercept of the relationship between viscosity and percent weathered (% of volatiles lost) being the initial viscosity. For emulsifying oils, after a combination of weathering and emulsification, oils eventually reached their maximum water content and viscosity (**Figure 2**).

These results show that the maximum water content is the controlling input parameter for modeling oil viscosity of emulsified oils. The maximum water content is set to zero if an oil does not emulsify, and for emulsifying oils, the magnitude of the maximum water content controls the ultimate viscosity of the oil emulsion.

Table 2 summarizes the results from this sensitivity study for the 13 oils, with oils of similar fate behaviors grouped together, listing viscosities at 20°C for 1) non-weathered, 2) fully weathered (assuming all volatiles and semi-volatiles to a boiling point of 380°C have evaporated) but not emulsified, and 3) both fully emulsified and fully weathered oils. If an oil does not emulsify (e.g., condensates, Bakken crude oil, and light fuels), the viscosity is controlled by the weathering and ambient temperature. If an oil emulsifies, the viscosity dramatically increases due to the uptake of water. The ultimate viscosities of emulsions were primarily a

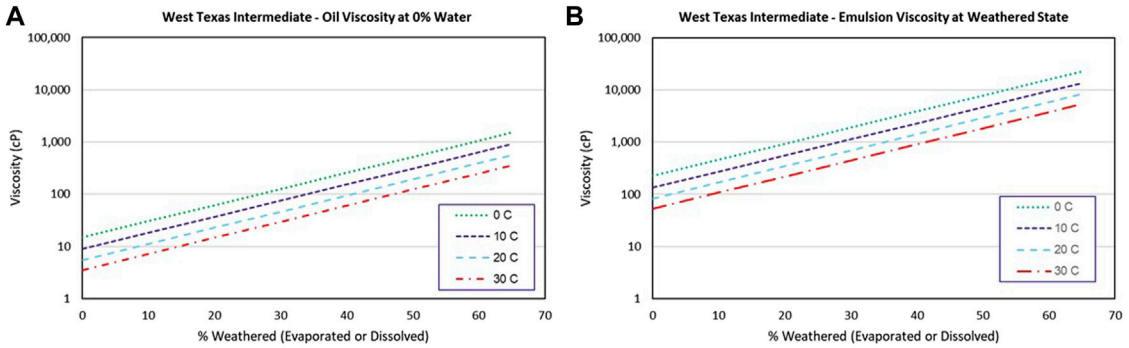

FIGURE 1 | Viscosity as a function of weathering, assuming no emulsification **(A)**, compared with viscosity of the fully emulsified oil at varying weathering states **(B)** for West Texas Intermediate oil.

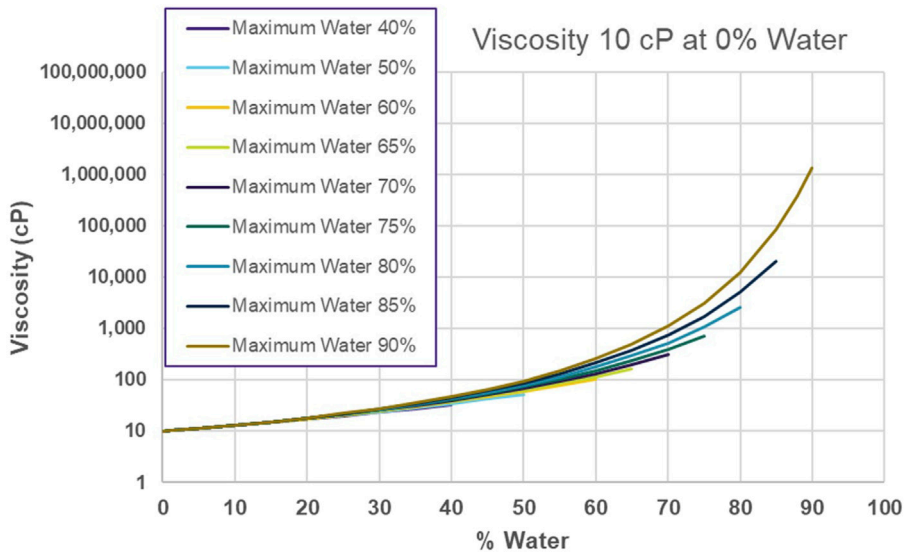

FIGURE 2 | Viscosity changes with water content for oils with an initial viscosity of 10 cP and varying maximum water content.

function of the maximum water content, but also influenced by the volatile content and initial viscosity.

The heavy—highly viscous oils (**Table 2**) were very viscous initially, and with weathering quickly became so viscous that they would not easily entrain into the water. Thus, emulsification would not change their behavior significantly. Whereas the heavy crudes (**Table 2**) have a low enough initial viscosity to entrain before weathering and emulsification occurs. Thus, the Western Canadian Select (WCS) oil was selected for further evaluation, as emulsification could affect this heavy oil's fate over-and-above the effect of weathering. The medium crude oils (**Table 2**) characterize oils with low volatile content and high emulsion water content. The sensitivity study showed that the effect of emulsification could substantially affect their oil fate, so Bow River Blend (BRB) was selected for analysis in phases 2 and 3. The Alaska North Slope (2017) crude (**Table 2**) is an unusual medium crude oil in that the emulsion had a very low maximum water content, while the light crude oils (**Table 2**) had high volatile content and low initial (fresh) viscosities. Emulsification dramatically changed the viscosities of these light crude oils. West Texas Intermediate (WTI) was the third oil selected for further analysis, representing the light crudes. The ultralight crudes and condensates (**Table 2**) do not emulsify, and so viscosities were controlled solely by weathering.

In the spill simulations for the representative oils, the rate of water uptake varied by oil type (determined by the maximum water content and the initial asphaltene and resin content) and with wind conditions (speeds). For WTI, the initial asphaltene and resin concentrations in the oil were low, so preliminary weathering was required to concentrate these components before water uptake initiated. WTI was fully emulsified after approximately 30 h of weathering and 3 days of water uptake in light winds (<5 m/s). In contrast, BRB and WCS began emulsifying immediately, reaching maximum water content in

TABLE 2 | Viscosity at 20°C for non-weathered, fully weathered[a] non-emulsified, and fully emulsified as well as fully weathered oils. (The classification and associated colors indicate oils of similar expected behavior).

Oil name	API	Classification	Max. % water	Fraction volatiles	Viscosity (cP) unweathered	Viscosity (cP) weathered	Viscosity (cP) emulsion
IFO380 Prestige	10.8	Heavy—highly	60.0	0.16	16,180	1,623,000	16,910,000
IFO180	14.9	viscous	69.0	0.32	1,385	138,800	3,736,000
Platform elly	15.8		64.0	0.37	2,311	231,700	3,483,000
Maya 2004	20.4	Heavy crudes	64.0	0.47	399	40,000	601,100
WCS 2017	**21.7**		**60.0**	**0.22**	**267**	**26,810**	**279,300**
Bow River Blend	**27.0**	Medium crudes	**66.0**	**0.47**	**28.0**	**2,807**	**52,230**
Petronius block VK786A	31.0		78.3	0.49	7.8	781	122,900
Alaskan North slope 2017	32.5	Low water	31.0	0.46	8.9	889	2,096
HOOPS	34.2	Light crudes	64.0	0.57	8.4	846	12,710
MC252 2020	35.4		64.0	0.62	5.8	585	8,800
West Texas Intermediate	**36.6**		**64.0**	**0.65**	**5.5**	**554**	**8,324**
Bakken crude	40.6	No emulsification	0.0	0.73	3.4	337	337
Oso condensate	49.2		0.0	0.82	1.6	157	157

[a]*Fully weathered is defined here as <1% left of the fraction boiling off by 380°C. These data are calculated by spreadsheet, and full weathering may not occur in the field. The bolded oils were selected for further evaluation in phases 2 and 3.*

light winds in approximately 36 and 12 h, respectively. At higher wind speeds (5–10 m/s), full emulsification was reached in a few hours for all three oils.

3.2 Phase 2: Probabilistic Oil Fate and Exposure Model Results

To evaluate the influence of emulsification processes on the fate and behavior of each oil type (WTI, BRB, and WCS), stochastic (probabilistic) modeling was performed by enabling 1) weathering only (i.e., F_{wmax} = 0) and 2) both weathering and emulsification processes. As expected, shoreline oiling was predicted to be minimal due to the release location being far offshore, while results for floating oil and water column exposures highlighted the influence of emulsification on the predicted fate and behavior of the hypothetical releases. Thus, results for floating oil and water column exposures are reported here.

Figure 3 maps the probabilities of surface oil exposure for the multiple model runs comprising the probabilistic scenario for WTI including emulsification. For this offshore location where the spill simulations were modeled, the currents were relatively weak and variable, with winds varying seasonally and over time, such that oil trajectories had nearly equal probabilities of moving in any direction on an annual basis. Based on the wind rose (**Supplementary Appendix Section A.1.2**, **Supplementary Appendix Figure A1**), easterly winds were stronger than westerlies, so oil moved faster when transported to the west. However, the stronger easterlies entrained and dispersed the oil more readily, such that the trajectories were of similar length in all directions. Similar maps for the other oils (**Supplementary Appendix Section A.2**; **Supplementary Appendix Figures A2–A6**) show that the extent of the trajectories increased with oil viscosity, either by nature of the fresh oil or especially with emulsification. Thus, more viscous oils remained on the surface and were more persistent.

Note that the areas exposed to surface floating oil and the volumes of water exposed above threshold concentrations are functions of the amount of oil assumed spilled. Larger areas and volumes affected above the thresholds would result from larger spills. Thus, while absolute differences in results between the runs with and without emulsification will vary by the spilled amount, patterns can be discerned by comparing the scenarios based on the example spill amount simulated (i.e., 200 MT of oil).

The probabilistic results are summarized in **Tables 3–7** and **Supplementary Appendix Tables A12–A21** in **Supplementary Appendix Section A.2**. The mean values reported in these tables are the expected values given a spill of 200 MT of oil, that would result for a range of weather conditions. They are calculated as the average result, based on the set of 114 model simulations evaluated for a single scenario, by varying the start date, and so the environmental conditions following the spill.

The modeling results are best understood by considering the viscosity of the surface oil at its most weathered state in the simulations. Emulsification significantly increased the viscosity of the floating oil, regardless of oil type, which ultimately changed the fate and behavior of the oil. For all oil types, viscosity decreased by about an order of magnitude between the simulations with and without emulsification (**Table 3**).

Tables 4, **5** summarize the surface areas swept by floating oil and water volumes exposed to dissolved concentrations >1 μg/L for each oil type. Water volumes exposed to dissolved concentrations >10 μg/L are in **Supplementary Appendix Table A12** in **Supplementary Appendix Section A.2**. The average exposures (as μg/L-hours) in the volumes of water affected by dissolved hydrocarbon concentrations ≥1 μg/L are summarized in **Table 6**.

Supplementary Appendix Tables A13–A16 summarize the mean and 95th percentile results of the mass balance for the 114 model simulations for each scenario, based on the maximum value at any time for each simulation. The maximum amount of

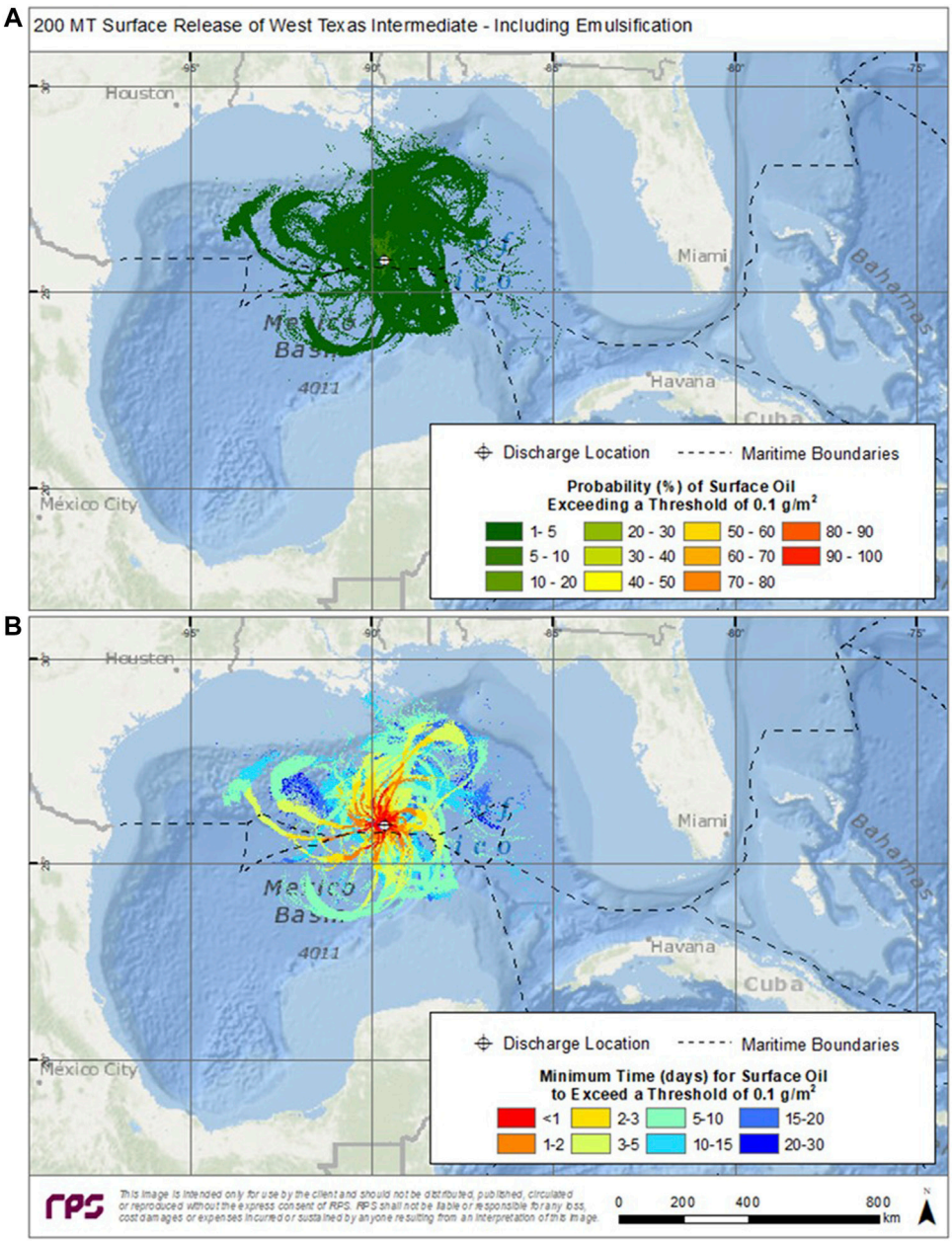

FIGURE 3 | (A) displays probability of surface oiling ≥0.1 g/m^2 and **(B)** displays minimum time for surface oil to exceed 0.1 g/m^2, based on a range of possible trajectories for a surface spill of 200 MT of WTI, including emulsification.

TABLE 3 | Expected viscosity (cP) of weathered floating oil for a surface release of 200 MT, based on results for 114 simulations varying spill date.

Emulsification condition	Metric	West Texas Intermediate	Bow River Blend	Western Canadian Select
With emulsification	Mean	6,432	33,700	79,150
	95th percentile	8,255	39,270	1,01,700
Without emulsification	mean	410	2,097	14,520
	95th percentile	510	2,452	18,600
Paired student's *t*-test	Probability not different	<0.01	<0.01	<0.01

TABLE 4 | Expected surface area (km^2) swept by ≥0.1 g/m^2 of floating oil for a surface release of 200 MT, based on results for 114 simulations varying spill date.

Emulsification condition	Metric	West Texas Intermediate	Bow River Blend	Western Canadian Select
With emulsification	Mean	9,670	45,220	38,420
	95th percentile	46,540	78,400	63,200
Without emulsification	Mean	1,306	17,920	55,660
	95th percentile	4,694	44,150	92,940
Paired student's *t*-test	Probability not different	<0.01	<0.01	<0.01

TABLE 5 | Expected water volumes (million m^3) exposed to dissolved concentrations ≥1 μg/L for a surface release of 200 MT, based on results for 114 simulations varying spill date.

Emulsification condition	Metric	West Texas Intermediate	Bow River Blend	Western Canadian Select
With emulsification	Mean	450	215	44
	95th percentile	703	426	119
Without emulsification	Mean	439	303	73
	95th percentile	671	509	170
Paired student's *t*-test	Probability not different	0.16	<0.01	<0.01

TABLE 6 | Expected exposure to ≥1 μg/L (1 ppb) dissolved concentrations, as the sum of concentration multiplied by duration of exposure (dose, μg/L-hours) over the simulation, for a surface release of 200 MT, based on results for 114 simulations varying spill date.

Emulsification condition	Metric	West Texas Intermediate	Bow River Blend	Western Canadian Select
With emulsification	Mean	327	260	74
	95th percentile	545	472	170
Without emulsification	Mean	361	202	81
	95th percentile	613	374	178
Paired student's *t*-test	Probability not different	<0.01	<0.01	<0.01

TABLE 7 | Percentage ultimately degraded or dispersed in the water column after a 200-MT spill, based on results for 114 simulations varying spill date.

Emulsification condition	Metric	West Texas Intermediate	Bow River Blend	Western Canadian Select
With emulsification	Mean	60.5	17.9	9.3
	95th percentile	76.9	37.3	20.2
Without emulsification	Mean	69.5	51.4	19.6
	95th percentile	77.1	69.0	41.7
Paired student's *t*-test	Probability not different	<0.01	<0.01	<0.01

surface oil occurred immediately after the spill; the maximum amount in the water column is typically within the first few days after the release; and the amounts in the atmosphere and degraded are cumulative by the end of the 30-day simulation. (Thus, the percentages do not add to 100%.) The maximum percentage on the water surface over the time of the simulation was higher for the more viscous oils (**Supplementary Appendix Table A13**, correlation with fresh oil viscosity was 0.997). The maximum percentages of oil evaporated, in the water column and degraded (**Supplementary Appendix Tables A14–A16**) were all inversely correlated with oil viscosity (correlation coefficients −0.74, −0.46, and −0.79, respectively), the dissolved mass percentages being highly correlated (−0.91) with viscosity. In **Supplementary Appendix Table A15**, the total in the water column includes weathered residuals formed from floating oil after evaporation was complete (defined as >99% of volatiles lost from the oil), assumed awash in the wave-mixed layer. As highly viscous but non-emulsified WCS became fully weathered (which did not occur by 30 days for emulsified BRB and WCS oils), the percentage of mass in the water column did not correlate with viscosity as much as did total dissolved mass.

In the first 30 days of the simulations, most of the degradation (biodegradation and photodegradation of PACs) occurred in the water column, and ultimately the mass in the water column at 30 days would biodegrade or settle. **Table 7** lists the total percentage that would ultimately be in the water column degraded, assuming no settlement. It is possible that some of the water column mass would settle to the sediments as part of marine snow, but in the 30-day time frame of these simulations, that settlement would not likely be significant.

Considerable percentages of the emulsified BRB and WCS oils, as well as WCS assuming no emulsification, remained floating as

partially weathered oil or as weathered residuals at 30 days (**Supplementary Appendix Tables A17, A18**; **Supplementary Appendix Section A.2**) because their high viscosities once weathered (>10,000 cP, **Table 3**) prevented entrainment. Emulsified BRB and WCS did not fully weather in 30 days, while all three oils fully weathered when emulsification was assumed not to occur. WTI with emulsification also fully weathered in <30 days. Ultimately, the floating oil would weather to become part of the weathered residual pool. **Supplementary Appendix Table A19** lists the total of remaining floating oil and weathered residuals at 30 days post-spill. For all three oils, emulsification resulted in more oil mass (not including the water in the emulsion) floating or remaining as weathered residuals than if emulsification did not occur.

The percentage in the water column at 30 days, without including the weathered residuals, was inversely correlated with viscosity (−0.77; **Supplementary Appendix Table A20**). The maximum percentage dissolved in the water column at any time occurred shortly after the spill when relatively fresh oil was entrained (inversely correlated with viscosity, −0.83; **Supplementary Appendix Table A21**). The total percentage of spilled oil that was dissolved or entrained and would ultimately be degraded in the water column (**Table 7**) decreased with the initial fresh oil viscosity. The percentage ultimately degraded in the water column increased when emulsification was prevented, by a factor of 2–3 for the BRB and WCS oils, and by 10% for WTI (which entrained readily even when emulsified). Results specific to each oil type are further described in the following subsections (**Sections 3.2.1–3.2.5**).

3.2.1 West Texas Intermediate

For the WTI (including emulsification), the model predicted a low likelihood for oil to move north over the US continental shelf or over the Yucatan shelf north of Mexico (**Figure 3**) because this light crude was easily entrained during stormy conditions. In some weather conditions (i.e., southerly winds), there was potential exposure to surface oil north of the spill site over the shelf. As for the weathered-only WTI modeling, the floating oil trajectories were much shorter (**Supplementary Appendix Figure A2**) because the oil viscosity remained low (**Table 3**) and the oil was easily entrained during windy periods.

When emulsification was included in the WTI simulations, on average, the floating oil fully weathered to a density ~1.0 and a viscosity of ~6,400 cP (**Table 3**), slowing entrainment. Whereas the non-emulsified floating oil fully weathered to a viscosity of <510 cP. Negating the emulsification slightly decreased the mass of volatiles evaporating (**Supplementary Appendix Table A14**) and increased the oil in the water column (**Supplementary Appendix Tables A15, A20, A21**) because the light WTI crude (without emulsification) was more easily entrained during stormy conditions than WTI with emulsification.

3.2.2 Bow River Blend

The stochastic footprint for the BRB (including emulsification) simulations were much larger (i.e., the oil was predicted to travel further) than the WTI scenarios, extending well into the continental shelf and reaching shorelines both north and west of the spill site (**Supplementary Appendix Figure A3**). This was due to the higher viscosity of BRB (**Table 3**) limiting entrainment into the water so that entrainment could only occur during stormy conditions. For the simulations when emulsification was included, the floating oil fully weathered to a density ~1.0 and a viscosity averaging ~34,000 cP, while a fully weathered (non-emulsified) BRB was predicted to have a much lower viscosity of ~2,000 cP (**Table 3**).

The BRB weathering-only trajectories (**Supplementary Appendix Figure A4**) were similar to the WTI scenarios (**Supplementary Appendix Figure A2**) in that the floating oil trajectories were much shorter when emulsification was excluded but differed from WTI in that there was a low probability of shoreline oiling. The smaller surface area footprint when emulsification was prevented was due to the oil viscosity remaining low (**Table 3**), which allowed oil to readily entrain during windy periods. Emulsification of BRB oil decreased the percentage of oil and dissolved oil components in the water column (**Supplementary Appendix Tables A15, A21**) and therefore increased the percentage of volatiles evaporating (**Supplementary Appendix Table A14**). This is because the BRB without emulsification was more easily entrained during stormy conditions than BRB with emulsification, where the oil remained at the surface.

3.2.3 Western Canadian Select

Oil trajectories for the WCS including emulsification (**Supplementary Appendix Figure A5**) were similar in size to the BRB scenario with emulsification, extending into the continental shelf and reaching shorelines both north and west of the spill site. Once again, this was due to the high viscosity of WCS (**Table 3**) inhibiting entrainment into the water. The floating oil fully weathered to a density ~1.0 and a mean viscosity of ~79,000 cP (**Table 3**). Unlike the WTI and BRB scenarios, many of the oil trajectories were similar regardless of the inclusion of emulsification (**Supplementary Appendix Figures A5, A6**). The maximum amount in the water column was substantially higher for the non-emulsified WCS (**Supplementary Appendix Table A15**), owing to its much lower viscosity (mean viscosity of ~14,500 cP, **Table 3**), allowing it to be dispersed into the water for a wider range of environmental conditions. However, due to its low volatile content (**Supplementary Appendix Tables A10, A11**) and lower viscosity (**Table 3**) allowing spreading, the non-emulsified WCS weathered (by evaporation) quickly, such that water column exposure to dissolved constituents was lower than for the emulsifying WCS (**Supplementary Appendix Tables A20, A21**). Some of the weathered-only trajectories traveled further (**Supplementary Appendix Figure A6** compared to **Supplementary Appendix Figure A5**) because the winds were enough to entrain fresh oil and transport it by currents (e.g., in the Loop Current) in a different direction from the wind forcing.

Biodegradation was facilitated by the entrainment and (natural) dispersion into the water column, but as entrainment of WCS was lower than for other oils, so was biodegradation (**Supplementary Appendix Table A16**). Negating the emulsification slightly decreased the mass of volatiles and so

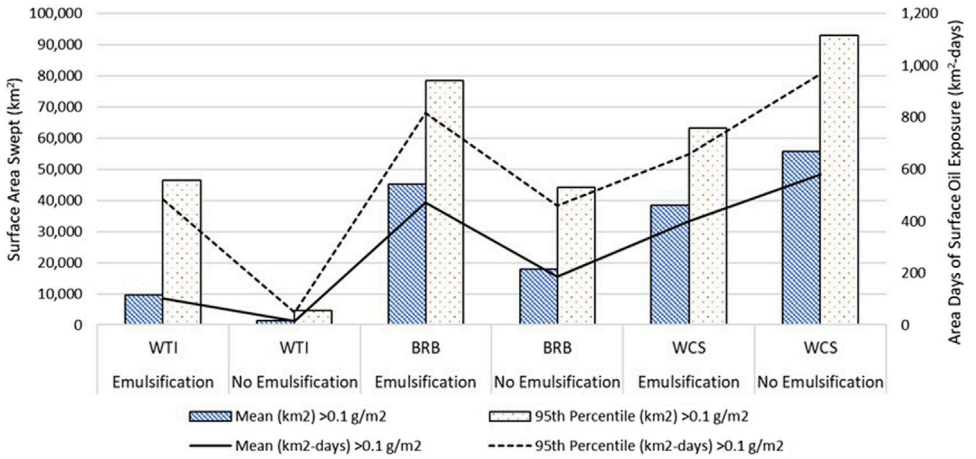

FIGURE 4 | The mean and 95th percentile surface area swept (km^2) and area-days of surface oil exposure (km^2-days) ≥0.1 g/m^2 threshold for each stochastic scenario (i.e., all oils with and without emulsification).

the percentage of the oil evaporating (**Supplementary Appendix Table A14**) because non-emulsified WCS was more easily entrained during stormy conditions than emulsified WCS.

3.2.4 Surface Area Exposure—All Oils

For all stochastic scenarios, the cumulative water surface areas exposed to oil ≥0.1 g/m^2 (**Table 4**) and ≥10 g/m^2 over the 30-days simulation, based on the swept areas of the Lagrangian Elements used to simulate the floating oil, were calculated for each model run (of the 114 simulations). As results were similar for the ≥0.1 g/m^2 and ≥10 g/m^2 thresholds, only the mean and 95th percentile results for the surface areas swept and area-days for floating oil exposure ≥0.1 g/m^2 are presented (**Figure 4**). The average duration of exposure was calculated by dividing the area swept each time step multiplied by time step, summed over all time in the simulation (km^2-days), by the summed area swept (km^2). Since the floating oil was continuously moving, the predicted average exposure duration for all stochastic modeling scenarios was approximately 15 min (i.e., one time step).

Except for the emulsified WCS, the water surface area swept by oil increased with increasing viscosity of the oil (**Table 4**), as higher viscosity decreased the rate of oil entrainment during windy periods. The correlation coefficients between the metrics summarizing surface oil exposures (water surface areas swept by oil and areas-days of floating oil exposure) and fresh oil viscosities were 0.73–0.74.

For WTI (including emulsification), the range of potential surface area exposed to ≥0.1 g/m^2 of floating oil was very broad, from just over 10 to nearly 90,000 km^2, depending upon the wind speeds following the release (**Supplementary Appendix Figure A7**; **Supplementary Appendix Section A.2**). The mean and 95th percentile simulations of WTI (including emulsification) were predicted to result in 9,670 km^2 and 46,500 km^2 of surface area swept by ≥0.1 g/m^2 of floating oil, respectively. For simulations including emulsification, the exposure area was predicted to be an order of magnitude larger than for weathered-only WTI and significantly different ($p < 0.01$) for both thresholds (**Table 4**; **Supplementary Appendix Figures A7, A9**). WTI including emulsification reached viscosities of ~10,000 (cP), whereas without including emulsification viscosities were at most ~600 (cP). Thus, without emulsification, the WTI (or any light crude that does not emulsify) is much more ephemeral on the water surface, entraining more easily after weathering such that the area exposed to floating oil is about 10 times less than for WTI with emulsification.

The BRB (including emulsification) simulations were predicted to have a potential surface area exposed to ≥0.1 g/m^2 of floating oil between ~16,000 and ~91,000 km^2, depending on environmental conditions during the spill (**Supplementary Appendix Figure A11**), higher than for WTI because of the higher viscosity of BRB (**Table 3**). Results for the weathered-only BRB predicted an order of magnitude decrease in the minimum value (2,440 km^2) and a slightly smaller maximum value (81,660 km^2) for the surface area swept by ≥0.1 g/m^2 of floating oil (**Supplementary Appendix Figure A13**). The mean and 95th percentile exposures were about 40% of what they were for BRB with emulsification and weathered-only BRB were predicted to have significantly ($p < 0.01$) smaller areas swept by floating oil with concentrations ≥0.1 g/m^2 (**Table 4**). Without emulsification, the BRB is more ephemeral on the water surface, entraining more easily than BRB with emulsification. Similar results would be expected for other medium crude oils that do not emulsify.

Depending on wind speeds after the spill, the range of potential surface area exposed to ≥0.1 g/m^2 of floating WCS (including emulsification) ranged from ~16,000 to ~71,000 km^2 (**Supplementary Appendix Figure A15**). Since weathered WCS is very viscous and because weathering occurred quickly, most of the surface oil was ≥10 g/m^2 (>10 μm thick), so the areas swept were essentially the same for ≥0.1 g/m^2 and ≥10 g/m^2 thresholds. The range of potential surface areas exposed to ≥0.1 g/m^2 of floating oil for the weathered-only WCS simulations was broad, from ~25,000 to

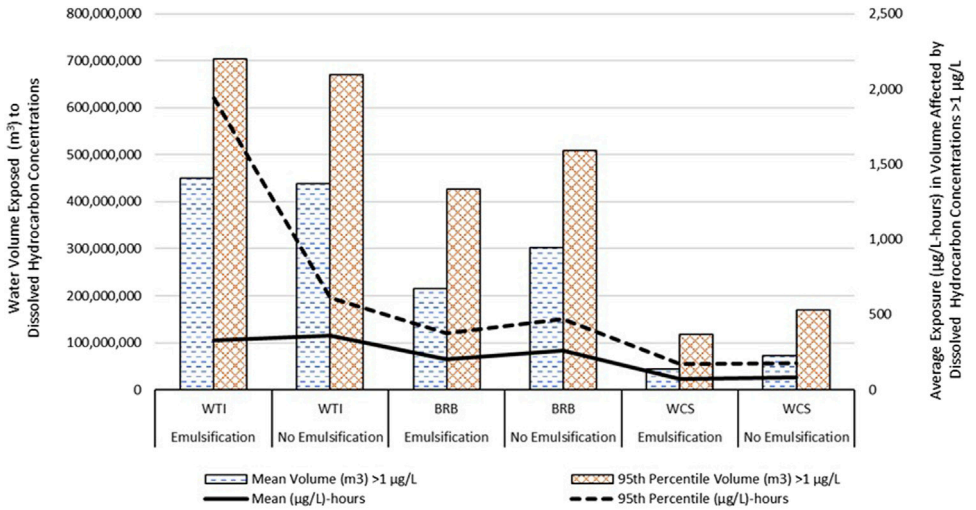

FIGURE 5 | The predicted water volume (m^3) exposed to dissolved hydrocarbon concentrations ≥1 µg/L and the average exposure (µg/L-hours) in the volume of water affected by dissolved hydrocarbon concentrations ≥1 µg/L for each oil type, with and without emulsification.

~106,000 km^2 (**Supplementary Appendix Figure A17**), and higher than the WCS (including emulsification) simulations (**Supplementary Appendix Figure A15**). The mean and 95th percentile exposures for weathered-only WCS were about 1.5 times larger than WCS with emulsification (**Table 4**). Without emulsification, the fresh WCS was more ephemeral on the water surface, entraining more easily. However, because the fresh oil was highly viscous to start with, the viscous oil entrained as large droplets, and resurfaced once the turbulence (i.e., winds) subsided. This expanded the area exposed to floating oil compared to WCS with emulsification because the entrained droplets were transported by subsurface currents differentially from the wind transport at the surface. For WCS, and other very viscous crude oils, the results indicate that emulsification as a weathering process may significantly decrease the potential surface area exposed to ≥0.1 g/m^2 or ≥10 g/m^2 of floating oil. However, the mass of crude oil remaining as floating oil or weathered residuals was much higher when emulsification was included (**Supplementary Appendix Tables A17–A19**).

3.2.5 Water Column Exposure—All Oils

Water column exposure was the second index used to evaluate and compare how the inclusion of emulsification when modeling a hypothetical oil spill can change its fate and behavior. Results for water column exposures were quantified as volume (m^3) exposed to dissolved hydrocarbon concentrations ≥1 µg/L (**Table 5**) and ≥10 µg/L (**Supplementary Appendix Table A12**), and the average and 95th percentile exposures (as µg/L-hours) in the volume of water affected by dissolved hydrocarbon concentrations ≥1 µg/L for each stochastic scenario (**Figure 5**). The volumes exposed were multiplied by duration exposure and summed to provide an index of exposure "dose" (i.e., µg/L-hours) that might be experienced by water column biota (**Table 6**). Water concentrations were highly variable over time and space. Dividing the minimum concentration in the volume, 1 µg/L (1 ppb), by dose indicates the maximum duration of exposure for any water parcel. Acute toxic effects are related to concentration and duration of exposure. For example, lethal concentrations to 50% of exposed organisms (LC50s) are higher with shorter durations of exposure, particularly for short (<24-hour) exposures (see reviews in French-McCay, 2002; French-McCay et al., 2022).

For all three oils, with or without emulsification, the water volume exposed to ≥10 µg/L was <0.001% of the volume exposed to concentrations ≥1 µg/L (**Table 5** and **Supplementary Appendix Table A12**). The volume of water affected by dissolved concentrations ≥1 µg/L decreased with higher viscosity of the oil or emulsion (**Figure 5**). This is because entrainment was inhibited by increased viscosity, both in terms of mass entrained and the residence time of the entrained oil underwater, allowing for dissolution to occur. However, there were some nuances to this pattern, depending upon the initial non-weathered oil viscosity.

For WTI (including emulsification), in 90% of potential spills (i.e., weather conditions), the volumes where maximum dissolved concentrations ≥1 µg/L (1 ppb) and ≥10 µg/L were 0.1–0.7 km^3 and 300–1,500 m^3, respectively (**Supplementary Appendix Figure A8**). Results were similar for the weathered-only WTI simulations as 90% of potential spills where maximum dissolved concentrations ≥1 µg/L (1 ppb) ranged from 0.1 to 0.7 km^3 and ≥10 µg/L ranged from 300 to 1,300 m^3 (**Supplementary Appendix Figure A10**). For WTI oil, including emulsification did not significantly affect the water volume exposed to dissolved concentrations ≥1 µg/L (**Table 5**) because dissolution occurred from relatively fresh oil, which had such low viscosity it was easily entrained, prior to emulsifying. For the weathered-only WTI, the water volumes exposed to concentrations ≥10 µg/L were significantly less than those with emulsification (**Supplementary Appendix Table A12**). However, this result was driven by two extremely high events for water exposures

with emulsification (**Supplementary Appendix Figure A8**). The non-emulsified oil, being spread thinner, had lost more of the PACs before the high wind events occurred. Thus, dissolution was limited, and so the peak concentrations were lower, for those two spill dates for the non-emulsified WTI (**Supplementary Appendix Figure A10**).

For the BRB (including emulsification), 90% of potential spills volumes where maximum dissolved concentrations ≥1 μg/L ranged from 0.001 to 0.4 km^3 and ≥10 μg/L ranged from 1,000 to 2,500 m^3 (**Supplementary Appendix Figure A12**). For weathered-only BRB simulations, the maximum dissolved concentrations at any time were ≥1 μg/L in volumes ranging from 0.1 to 0.5 km^3 for 80% of the potential spills (**Supplementary Appendix Figure A14**), which was slightly larger than when emulsification occurred. For BRB with or without emulsification, the water volume exposed to ≥10 μg/L (**Supplementary Appendix Table A12**) was <0.001% of the volume exposed to concentrations ≥1 μg/L (**Table 5**). Without emulsification, the water volumes exposed to dissolved concentrations ≥1 μg/L increased by 41% on average (**Table 5**) and the volumes ≥10 μg/L decreased by a factor of two (**Supplementary Appendix Table A12**), as compared to the emulsifying oil. This occurred for the non-emulsified oil because entrainment and resulting dissolution occurred over a broader area since the oil spread further and remained of low enough viscosity to entrain much longer than the emulsifying oil. For most model runs, the water column dissolved concentrations for BRB without emulsification resulted from repeated entrainment events, followed by resurfacing, whereas for BRB assuming emulsification, entrainment was restricted to soon after the spill before the oil emulsified and became too viscous to entrain. This led to smaller volumes with higher dissolved concentrations when emulsification was included.

Results for WCS (including emulsification), showed that for 90% of potential spills, volumes where maximum dissolved concentrations ≥1 μg/L ranged from 0.05 to 0.1 km^3 and ≥10 μg/L ranged from 1,400 to 2,400 m^3 (**Supplementary Appendix Figure A16**). The maximum dissolved concentrations at any time were ≥1 μg/L in volumes ranging from 0.05 to 0.2 km^3 for 56% of the potential spills (i.e., weather conditions) for WCS without emulsification (**Supplementary Appendix Figure A18**), higher than WCS with emulsification (**Supplementary Appendix Figure A16**; **Table 5**). For WCS, the emulsification did not greatly change the volume exposed to ≥10 μg/L dissolved concentration (**Supplementary Appendix Figures A16, A18**; **Supplementary Appendix Figure A12**) and that volume was <0.001% of the volume exposed to concentrations ≥1 μg/L. The emulsification resulted in a 66% (on average) smaller volume of water exposed to concentrations ≥1 μg/L because there was much less entrainment as that oil weathered and became highly viscous.

The dose metric μg/L-hours (the sum of concentration multiplied by duration of exposure) in **Table 6** provides an integrated index of exposure to dissolved concentrations ≥1 μg/L. The dose decreased with increasing fresh oil viscosity. For WTI and WCS, the integrated exposure dose indices increased when emulsification was prevented, whereas for BRB the opposite trend resulted. For WTI, the non-emulsifying oil easily and repeatedly entrained, and so water exposure was higher than for the emulsifying oil that became more viscous in time. For BRB, while the non-emulsifying oil repeatedly entrained, it did so less easily and spent more time exposed to evaporation than WTI (**Supplementary Appendix Figure A14**). The oil entrained over a broader area and diluted more than the WTI. Thus, the exposure dose was lower for BRB than for WTI. Dissolved concentrations from emulsified BRB were higher in a smaller volume than for non-emulsifying BRB. The integrated exposure dose for WCS was higher without emulsification because more of the oil could entrain and dissolve.

3.3 Phase 3: Deterministic Oil Fate and Exposure Model Results

Two individual deterministic model simulations from each of the six stochastic scenarios are examined in further detail in this section to investigate the effect of emulsification on oil weathering and mass balance (i.e., entrainment, dissolution, and biodegradation). The 95th percentile for surface oil exposure and 95th percentile for water column exposure were selected from the set of runs performed for the scenario including emulsification. The runs with the same spill dates were examined for the paired scenario (i.e., with and without emulsification) for the same oil type (**Supplementary Appendix Table A22**). Maps showing the oil trajectories are in **Supplementary Appendix Section A.2** (**Supplementary Appendix Figures A19–A30**). Mass balance plots of the amount of oil in each environmental compartment (i.e., on the surface, in the atmosphere, in the water column, on the shoreline, etc.,) over time are shown in **Figures 6–8** for the example deterministic simulations.

3.3.1 West Texas Intermediate

The maximum water surface oil exposure for the spill date that led to the 95th percentile for surface oil exposure (including emulsification), was smaller for the run without emulsification. The initial trajectory was similar, with high concentrations (>100 g/m^2) extending roughly 80 km south, however the lower concentrations (<1 g/m^2) did not extend as far (**Supplementary Appendix Figure A19**). The maximum water column dissolved concentrations were also similar for spills with or without emulsification (**Supplementary Appendix Figures A19, A21**) because the dissolution occurred primarily from very low viscosity oil that was entrained in the water column soon after it was released.

For the spill date that led to the 95th percentile for water column exposure (including emulsification), the maximum water column dissolved concentrations were nearly identical between the emulsifying oil and oil not including emulsification (**Supplementary Appendix Figures A20, A22**). Again, this resulted from entrainment directly after the spill occurred. The plumes traveled directly west with lower concentrations reaching approximately 75 km. The maximum surface oil exposure for both simulations, with and without emulsification, were negligible as the oil was entrained immediately by high winds at the time of the spill.

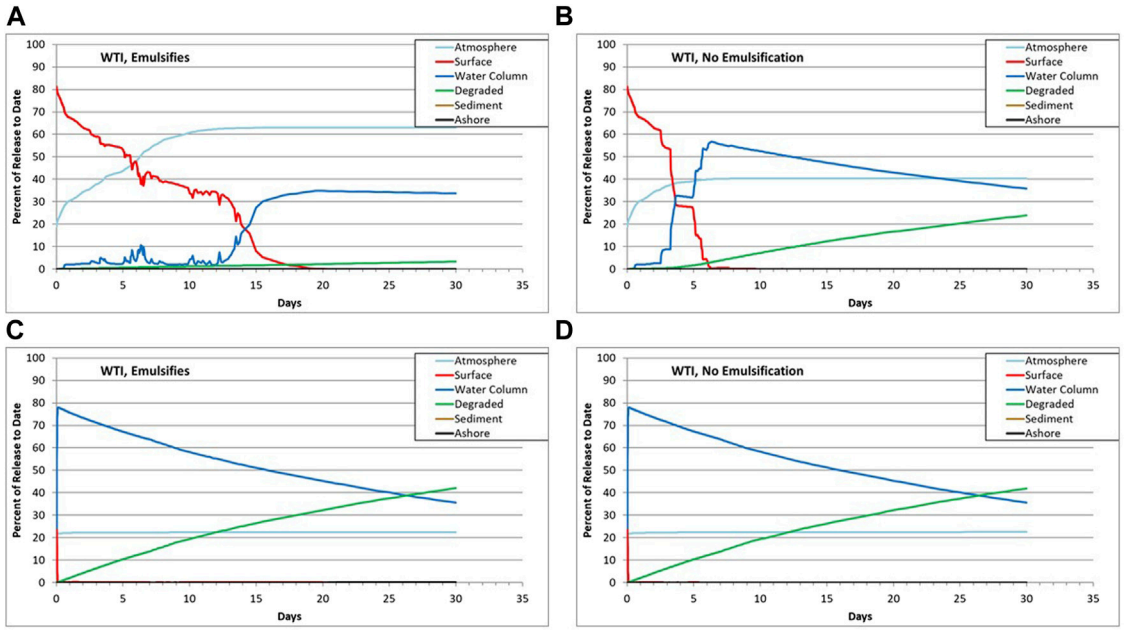

FIGURE 6 | Mass balance (as percent of the spilled mass) for a surface release of 200 MT of WTI for the runs that led to the 95th percentile for surface oil exposure [**(A,B)**; 15 June 2008] and for water column exposure [**(C,D)**; 15 December 2008], including emulsification **(A,C)** and not including emulsification **(B,D)**.

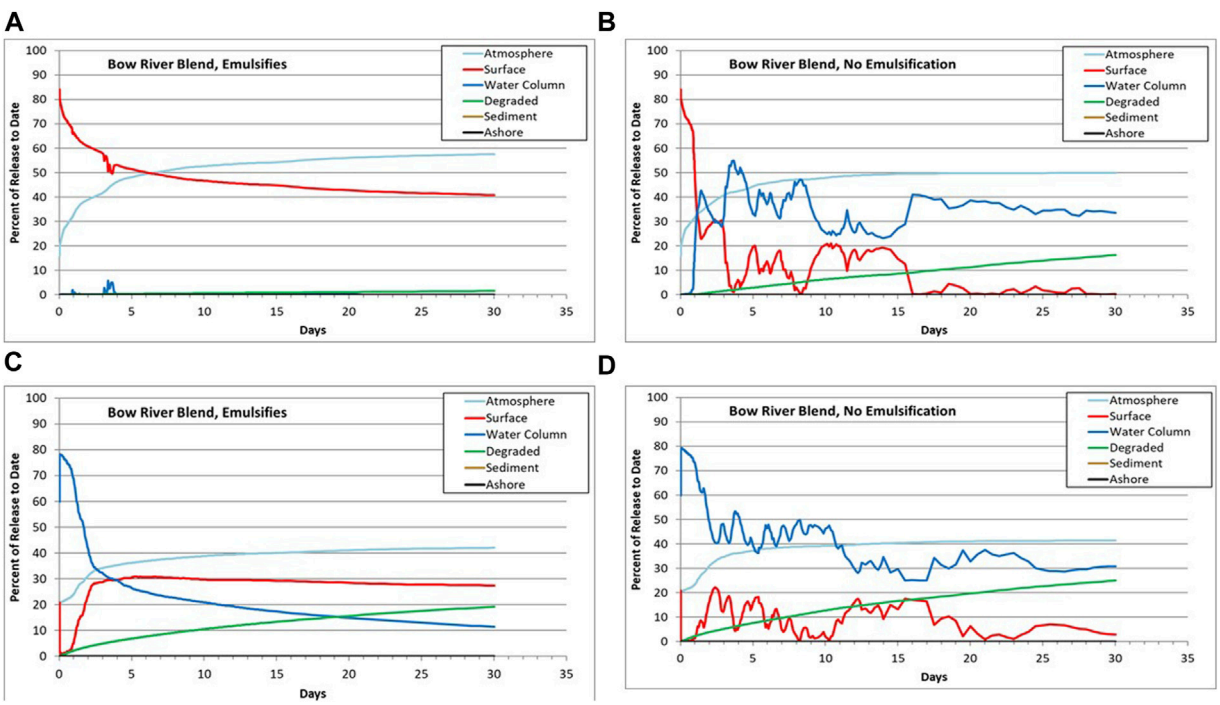

FIGURE 7 | Mass balance (as percent of the spilled mass) for a surface release of 200 MT of BRB for the runs that led to the 95th percentile for surface oil exposure [**(A,B)**; 1 October 2009] and for water column exposure [**(C,D)**; 15 April 2007], including emulsification **(A,C)** and not including emulsification **(B,D)**.

The mass balance over time for the four simulations of WTI spills with and without emulsification (95th percentile for surface area swept, and 95th percentile for water column exposure, **Figure 6**) shows that more oil was entrained into the water when winds and waves were higher. The winds and waves were much higher in December 2008 (the 95th percentile for water

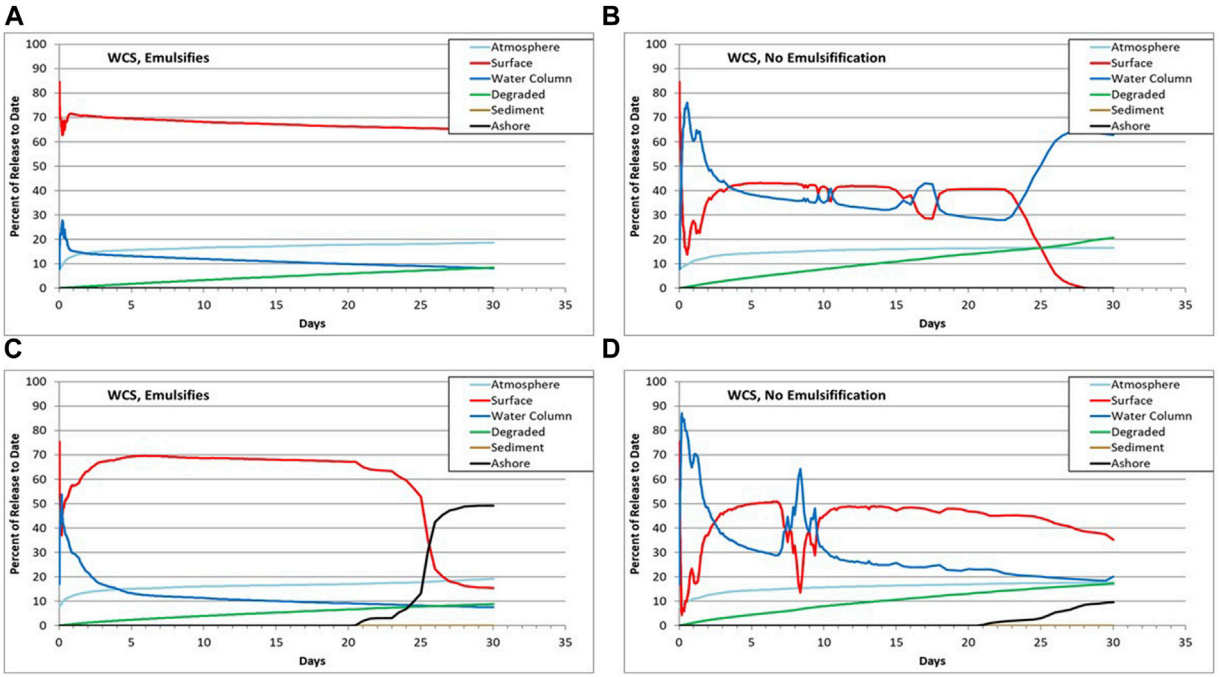

FIGURE 8 | Mass balance (as percent of the spilled mass) for a surface release of 200 MT of WCS for the runs that led to the 95th percentile for surface oil exposure [**(A,B)**; 15 August 2008] and for water column exposure [**(C,D)**; 15 May 2008], including emulsification **(A,C)** and not including emulsification **(B,D)**.

column exposure simulation; **Figures 6C,D**) than in June 2008 (the 95th percentile for surface area swept simulation; **Figures 6A,B**), so that with emulsification floating oil persists for about 19 days after the June 15th spill (**Figure 6A**) and <1 day after the December 15th spill (**Figure 6C**). The spill dates, and so the wind and wave conditions at the spill site, for the runs without emulsification were the same as for the scenario with emulsification. As occurred when the oil emulsified, the weathered-only WTI floating oil was entrained into the water much faster in December 2008 (**Figure 6D**), when winds and waves were higher than in June 2008 (**Figure 6B**), when winds were light. Because in the December run entrainment was complete within hours, there is little difference between results with and without emulsification (**Figures 6C,D**). However, for the June run, when winds were light, the non-emulsifying oil entrained much faster than when it emulsified, owing to order-of-magnitude lower viscosity without emulsification, and this is reflected in the mass balance of the two runs (**Figures 6A,B**). Weathering occurred much more rapidly with the higher winds during the 95th percentile run for water column exposure.

Due to high entrainment, the areas exposed to floating oil were much less for the December run with the higher water column exposure, as indicated by the mass balance (**Figure 6**). The volatiles (MAHs = total monoaromatics, which includes BTEX = benzene, ethylbenzene, toluene and xylenes, and soluble alkanes = C_5 to C_{10} alkanes) evaporate much faster than the semi-volatile PACs from floating oil, and evaporation is faster during higher winds. For WTI simulations (including emulsification), BTEX and other volatiles were depleted from the oil in less than 24 h, whereas PAC concentrations in the oil decreased to <1% by 11 days (95th percentile run for surface area swept) and 17 days (95th percentile run for water column exposure) after the spill, at which point the oil was considered to be weathered residuals awash in the surface wave mixed layer, and counted as part of the water column mass.

For the weathered-only WTI simulations, evaporative losses of volatiles and PACs were faster for the weathered-only oil than when emulsification was included because the weathered oil spread thinner. BTEX and other volatiles were depleted from the oil in less than 24 h and PAC concentrations in the oil decreased to <1% by 8 days (95th percentile run for surface area swept) and 6 days (95th percentile run for water column exposure) after the spill, after which the oil was considered weathered residuals and counted as part of the water column mass.

3.3.2 Bow River Blend

For BRB simulations (including emulsification), the maximum water surface oil exposure footprint of the run that led to the 95th percentile for surface oil exposure circled clockwise from the discharge location, due to the currents at the time indicating the presence of a large anticyclonic eddy. The highest concentrations (>500 g/m^2) extended northeast approximately 150 km (**Supplementary Appendix Figure A23**). The maximum surface oil exposure concentrations for the non-emulsifying oil, for the spill date that led to the 95th percentile for surface oil exposure with emulsification (**Supplementary Appendix Figure A25**), were similar to the run including emulsification

(**Supplementary Appendix Figure A23**), traveling in a circular pattern in the anticyclonic eddy. However, in the run not including emulsification the surface oil did not have patches spreading north. Comparing the floating oil trajectories to the water column plumes for both of these simulations, one observes that the dissolved concentrations originated from oil dispersed soon after the spill. The maximum water column dissolved concentrations for BRB without emulsification were 1–10 μg/L in several locations below the surface oil trajectory (**Supplementary Appendix Figure A25**), resulting from repeated entrainment events, whereas they were minimal for the run with emulsification, resulting only from some minor entrainment immediately after the spill (**Supplementary Appendix Figure A23**).

For the spill date that led to the 95th percentile for water column exposure, the maximum water column concentrations with and without emulsification had the same initial trajectories (**Supplementary Appendix Figures A24, A26**), but the weathered-only oil entrained more readily than the emulsified oil. Excluding emulsification resulted in a smaller exposure footprint because the weathered-only BRB oil spread much thinner, and the semi-soluble PACs evaporated faster, and so some of the PACs did not get entrained and dissolved.

The mass balance plots over time for the four simulations of BRB spills with and without emulsification are shown in **Figure 7**. As with the WTI simulations, much more BRB oil was entrained into the water when winds and waves were higher, and this is reflected when comparing the mass balances for the four runs. The high winds and waves in the first days after the April 2007 spill entrained the relatively fresh oil as small droplets prior to it emulsifying, so oil remaining in the water column at day 2 persisted for the remainder of the simulation (i.e., it permanently dispersed; **Figure 7C**). In October, the relatively low wind and waves in the beginning of the simulation resulted in a higher percentage of floating oil and emulsions remaining on the surface throughout the entire 30-day simulation (**Figure 7A**). As for the emulsifying oil, the non-emulsifying floating oil was entrained into the water much faster on 15 April 2007, when winds and waves were very high at the beginning of simulation (**Figure 7D**), than after 1 October 2009, when winds were light for the first 15 days (**Figure 7B**). In October, entrainment was minimal when including emulsification (**Figure 7A**), however the non-emulsifying oil entrained to a much higher degree even with the relatively light winds seen in the first 15 days of the simulation (**Figure 7B**) due to its much lower viscosity. In April the high winds and waves immediately after the spill resulted in rapid entrainment for runs with and without emulsification, but the weathered-only simulation (**Figure 7D**) resulted in a greater percentage of oil remaining in the water column (because of smaller droplet sizes due to lower viscosity) than when emulsification was included (**Figure 7C**). In both runs without emulsification (**Figures 7B,D**), the oil readily entrained with each relatively high wind event, and resurfaced in each calm period, such that the amount of floating oil and oil in the surface water oscillated, reflecting each other. The oscillations did not occur with emulsification (**Figures 7A,C**).

The volatiles [MAHs and soluble (C_5 to C_{10}) alkanes] evaporated much faster than the semi-volatile PACs from floating oil, and PAC evaporation was slowed when the oil emulsified, becoming viscous and thick, reducing surface area. When including emulsification, BTEX and other volatiles were depleted from the oil in less than 24 h, whereas PAC concentrations in the oil remained >1% at 30 days after the spill for the examined (and all) model runs. Thus, with emulsification, the model predicted that it would take >30 days to form weathered residuals and the water column showed continually decreasing percentages (**Figures 7A,C**). Whereas, when emulsification was excluded and oil was spread thinner due to lower viscosity, BTEX and other volatiles were depleted from the oil in less than 24 h and PAC concentrations in the oil decreased to <1% by 9 days (95th percentile run for surface area swept) and 16 days (95th percentile run for water column exposure) after the spill, after which the oil was considered weathered residuals in the water column (**Figures 7B,D**).

3.3.3 Western Canadian Select

The water surface oil footprint of the simulation starting in August 2008 (**Supplementary Appendix Table A22**) that led to the 95th percentile for surface oil exposure circled clockwise from the discharge location (both with and without emulsification, **Supplementary Appendix Figures A27, A29**), due to the currents at the time indicating the presence of a large anticyclonic eddy. The WCS oil being more persistent than BRB oil, circled twice around this eddy, which was of similar size to that in October of 2009 (which transported the BRB, compare to **Supplementary Appendix Figures A23, A25**). For the WCS simulations with and without emulsification, the water column exposure occurred under the initial portion of the floating oil trajectory, followed the anticyclonic eddy about 150 km south (**Supplementary Appendix Figures A27, A29**).

For the run that led to the 95th percentile for water column exposure, both with and without emulsification, the floating oil and the water exposed to ≥1 μg/L first moved to the northwest, and then followed an anticyclonic (clockwise flowing) eddy extending further northwest (**Supplementary Appendix Figures A28, A30**). The maximum dissolved concentrations were more extensive for the spill without emulsification than with emulsification. While the floating oil exposure without emulsification was not as persistent as that with emulsification, it followed the same initial trajectory around the anticyclonic eddy. (Compare **Supplementary Appendix Figure A30** for without emulsification to **Supplementary Appendix Figure A28** for with emulsification).

The mass balances over time for the four simulations of WCS spills (95th percentile for surface area swept and 95th percentile for water column exposure, with and without emulsification) are shown in **Figure 8**. As with the other simulations, more oil was entrained into the water when winds and waves were higher, and this is reflected in the mass balance. The winds the first day after the spill were higher on 15 May 2008 (**Figures 8C,D**), than on 15 August 2008 (**Figures 8A,B**), so more entrainment was seen in the first day of the May simulations. In both simulations assuming the WCS emulsified, high waves and winds after day 6 do not result in any further entrainment due to the weathering

and emulsification of the oil that occurred in the first few days after the spills (**Figures 8A,C**). For the non-emulsifying oil in the August 2008 simulation (**Figure 8B**), the movement of floating oil into the water column between days 23 and 28 was due to the oil being so weathered (i.e., >99% of the volatiles and semi-volatiles were lost to evaporation, dissolution, and degradation) that the floating oil became weathered residuals, which in the model are considered as awash in the surface wave layer. In both the August and May runs without emulsification, oscillation between surface floating oil and entrained WCS oil is observed (**Figures 8B,D**) during high wind events due to the lower viscosity of the oil. Emulsified WCS did not show his behavior (**Figures 8A,C**). The non-emulsified weathered-only BRB had shown more frequent entrainment events (**Figures 7B,D**) due to its lower viscosity than weathered-only WCS (**Figures 8B,D**).

For simulations with and without emulsification, BTEX and other volatiles were depleted from the oil in less than 24 h. PAC and other semi-volatile concentrations in the oil including emulsification remained >1% at 30 days after the spill for the examined (and all) model runs, whereas semi-volatile concentrations in the weathered-only oil decreased to <1% by 23 days (95th percentile run for surface area swept) and 30 days (95th percentile run for water column exposure) after the spill, after which the oil was considered weathered residuals. Evaporative losses of volatiles and PACs were faster when no emulsification occurred than with emulsification because the non-emulsified oil was much less viscous and spread thinner.

4 DISCUSSION AND CONCLUSION

Findings from this study highlighted the importance of considering emulsification as a weathering process, as emulsification was shown to greatly influence the trajectory and fate of a spilled oil at sea. For the simulations when emulsification was included, the uptake of water was predicted to occur within hours to a few days, and as water content increased the viscosity increased dramatically. For all oils, as the viscosity increased, floating oil did not spread as thin on the water surface which slowed weathering processes associated with slick surface area (e.g., evaporation). Additionally, higher viscosity reduced entrainment of oil into the water and created larger droplets which resurfaced faster, consequently reducing the residence time in the water column and the potential for dissolution and biodegradation. An increase in the area exposed to floating oil was predicted to occur for the light (WTI) and medium (BRB) crudes when emulsification was included in the model because the increased viscosity reduced entrainment. Whereas, for the heavy oil (WCS), the area of surface oil exposure decreased somewhat when emulsification was included because the non-emulsified oil entrained into the water column during high wind events and resulting droplets were relatively large and resurfaced further away from the spill site once wind speed decreased.

As demonstrated here and in general, water column exposure to dissolved concentrations decreased with higher viscosity oils. Minimal differences in water volume exposure were predicted for the light oil (WTI) whether it emulsified or not, as much of it entrained prior to water uptake and the rapid increase in viscosity. In contrast, for the medium (BRB) and heavy (WCS) crudes, a decrease in the volume of water exposed to dissolved concentrations (above the thresholds of concern) was predicted to occur if the oil emulsified because entrainment was reduced by the oil's increased viscosity. Most toxic effects of oil on aquatic biota are due to dissolved soluble and semi-soluble (primarily PAC) components. As demonstrated by the model, the main dissolution pathway was via dispersed oil droplets rather than surface slicks because evaporation proceeded faster than dissolution from slicks. The higher the wind speed (and turbulence) and the lower the oil viscosity, the more oil was entrained, and the droplet sizes were smaller. While the droplets were underwater, dissolution occurred. The smallest oil droplets remained entrained in the water column for an indefinite period, and larger oil droplets rose to the surface at varying rates. Thus, most dissolution occurred from small droplets formed from low viscosity and relatively non-weathered oil. Alternatively, if an oil evaporated before it was entrained, exposure to the water column was reduced. Therefore, emulsification, through its influence on viscosity, prolonged exposure to floating oil by slowing or preventing it from dispersing in the water column, thus decreasing water column exposure.

The first phase of this analysis was performed to capture the most influential model parameters when simulating oil emulsification, these included: 1) whether the oil emulsifies or not; 2) the initial oil viscosity and density; 3) asphaltene and resin concentrations as these determine the needed weathering to allow emulsification; and 4) the maximum water content because this influences the oil viscosity. More accurate information on an oil's maximum water content would improve predictions of the fully emulsified oil's viscosity.

In the modeling performed here, the emulsions were assumed stable over the 30-day simulation. Emulsion stability under field conditions has not been quantified to the extent that it can be mechanistically predicted in an oil spill model (French-McCay et al., 2021a). The degree to which emulsion stability decreases over time while at sea would influence the floating oil exposures predicted herein, as well as spill response options and effectiveness. However, water column exposures to dissolved concentrations are determined within a few days of oil release, and as such would not be affected by differences in long-term stabilities of the emulsions. In addition, photo-oxidation and its influence on emulsification were not included in this analysis at this time but has the potential to expedite the weathering and emulsification process under favorable environmental conditions (e.g., long duration of exposure to sunlight).

The implications of emulsification on response effectiveness are clear as it dramatically changes oil volume (*via* water uptake) and viscosity. Increased viscosity affects mechanical removal rates, and the additional oil volume affects mechanical removal capacities. Dewatering would decrease the emulsion volume but involve additional disposal considerations and logistics. The changes in water content and viscosity affect the choices of mechanical equipment used, as well as decisions regarding other spill response options, such as use of herders, *in-situ* burning, and dispersant use (National Oceanic and Atmospheric Administration (NOAA), 2010; IPIECA, 2015; ITOPF, 2018).

Given the sensitivity of viscosity to emulsification, and oil fate to viscosity, understanding and quantification of oil

emulsification is an important area of research. To improve modeling oil emulsification, further experimental and observational data is needed. The first priority is to determine whether an oil emulsifies, and this dependence on the physical and chemical properties of the oil and how these change with weathering (i.e., evaporation, photo-oxidation). Experimental analysis should include a wide matrix of oil types, exposed to variable temperatures, turbulence, and light conditions. From these experiments, the following information should be reported: 1) identifying if, and when the oil forms a water-in-oil emulsion; 2) measurements characterizing bulk properties (viscosity, density, and interfacial tension) and chemical composition (e.g., asphaltenes, resins, wax content, gas chromatography, and oxygen content) as the oil weathers and emulsifies; 3) measurement of water content over time; 4) water-in-oil emulsion formation rate; 5) maximum water content in the emulsion; and 6) an evaluation of stability of emulsions once formed using (for example) water droplet size distribution, bulk properties (viscosity, interfacial tension, and density), and spreading tests (Zhao et al., 2022). At a minimum, items 1), 2), and 5) need to be reported to be useful for model development. Further research on oil emulsification processes (including influences of photo-oxidation), and coordination between researchers and modelers to incorporate findings into oil spill models, will improve predictions of oil trajectories and the fate and behavior of the spilled oil to better inform response operations, environmental impact assessments, and natural resource damage assessments.

DATA AVAILABILITY STATEMENT

The original contributions presented in the study are included in the article/**Supplementary Material**, further inquiries can be directed to the corresponding author.

AUTHOR CONTRIBUTIONS

DF-M designed the study. DF-M, MF, and MG analyzed the data. DF-M and MG wrote the manuscript. All authors listed have made a substantial, direct and intellectual contribution to the work, and approved it for publication.

FUNDING

This research was supported by Chevron Energy Technology Company, San Ramon, CA. Preparation of the manuscript and funds for open access publication fees were supported by the "Inter-laboratory Comparison of Protocols for Oil Emulsification" study funded by Fisheries and Oceans Canada, Multi-Partner Research Initiative (MPRI; contract number MECTS#4266483-MPRI 2021-009), *via* subcontract to New Jersey Institute of Technology, Newark, NJ, United States, NJIT Index: 997740.

ACKNOWLEDGMENTS

Amanda Bess, Don Danmeier, and Lyman Young are thanked for their review and insights in support of this study. The authors appreciate insightful and helpful comments made by reviewers. Responding to those comments improved the content of this manuscript.

SUPPLEMENTARY MATERIAL

The Supplementary Material for this article can be found online at: https://www.frontiersin.org/articles/10.3389/fenvs.2022.908984/full#supplementary-material

REFERENCES

Bonn Agreement (2009). Bonn Agreement Aerial Operations Handbook, 2009. London, UK. Available at: http://www.bonnagreement.org/site/assets/files/1081/ba-aoh revision 2 april 2012-1.pdf (Accessed June 4, 2015).

Bonn Agreement (2011). Bonn Agreement Oil Appearance Code Photo Atlas. Available at: http://www.bonnagreement.org/site/assets/files/1081/photo_atlas_version_20112306-1.pdf (Accessed April, 2017).

Chassignet, E. P., and Srinivasan, A. (2015). Data Assimilative Hindcast for the Gulf of Mexico. Report for US Department of the Interior. Sterling, VA: Bureau of Ocean Energy Management. OCS Study BOEM 2015-035, 40.

Daling, P. S., and Brandvik, P. J. (1988). "A Study of the Formation and Stability of Water-In-Oil Emulsions," in Proceedings of the Eleventh AMOP Technical Seminar on Environmental Contamination and Response, Vancouver, BC, June 7–9, 1988 (Ottawa, ON: Environment Canada), 153–170.1

Daling, P. S., Leirvik, F., Almås, I. K., Brandvik, P. J., Hansen, B. H., Lewis, A., et al. (2014). Surface Weathering and Dispersibility of MC252 Crude Oil. *Mar. Pollut. Bull.* 87, 300–310. doi:10.1016/j.marpolbul.2014.07.005

Fingas, M., and Fieldhouse, B. (2014). "Chapter 8. Water-In-Oil Emulsions: Formation and Prediction," in *Handbook of Oil Spill Science and Technology*. Editor M. F. Fingas. First Edition (Hoboken, NJ: John Wiley & Sons), 225–270.

Fingas, M., and Fieldhouse, B. (2005). "How to Model Water-In-Oil Emulsion Formation, 2005," in Proceedings of the International Oil Spill Conference, 2005, 647–654. doi:10.7901/2169-3358-2005-1-647

Fingas, M., Fieldhouse, B., and Mullin, J. V. (1997). "Studies of Water-In-Oil Emulsions: Stability Studies," in Proceedings of the Twentieth AMOP Technical Seminar on Environmental Contamination and Response, Vancouver, BC, June 11–13, 1997 (Ottawa, ON: Environment Canada), 2142.1

Fingas, M., Fieldhouse, B., and Mullin, J. (1995). Water-in-oil Emulsions: How They Are Formed and Broken. *Proc. Int. Oil Spill Conf.* 1995, 829–830. doi:10.7901/2169-3358-1995-1-829

Fingas, M., and Fieldhouse, B. (2012). Studies on Water-In-Oil Products from Crude Oils and Petroleum Products. *Mar. Pollut. Bull.* 64, 272–283. doi:10.1016/j.marpolbul.2011.11.019

French-McCay, D., Crowley, D., Rowe, J. J., Bock, M., Robinson, H., Wenning, R., et al. (2018c). Comparative Risk Assessment of Spill Response Options for a Deepwater Oil Well Blowout: Part I. Oil Spill Modeling. *Mar. Pollut. Bull.* 133, 1001–1015. doi:10.1016/j.marpolbul.2018.05.042

French-McCay, D. (2003). Development and Application of Damage Assessment Modeling: Example Assessment for the North Cape Oil Spill. *Mar. Pollut. Bull.* 47 (9-12), 341–359. doi:10.1016/S0025-326X(03)00208-X

French-McCay, D., Horn, M., Li, Z., Crowley, D., Spaulding, M., Mendelsohn, D., et al. (2018b). *Simulation Modeling of Ocean Circulation and Oil Spills in the Gulf of Mexico, Volume III: Data Collection, Analysis and Model Validation.*

New Orleans, LA: US Department of the Interior, Bureau of Ocean Energy Management, Gulf of Mexico OCS RegionOCS Study BOEM 2018-041, 313.

French-McCay, D., Jayko, K., Li, Z., Horn, M., Isaji, T., and Spaulding, M. L. (2018a). "Volume II: Appendix II - Oil Transport and Fates Model Technical Manual," in *Simulation Modeling of Ocean Circulation and Oil Spills in the Gulf of Mexico*. Editors C. W. Galagan, D. French-McCay, J. Rowe, and L. McStay (New Orleans, LA: Prepared by RPS ASA for the US Department of the Interior, Bureau of Ocean Energy Management, Gulf of Mexico OCS Region, OCS Study BOEM 2018-040), 422.

French-McCay, D. P. (2002). Development and Application of an Oil Toxicity and Exposure Model, OilToxEx. *Environ. Toxicol. Chem.* 21 (10), 2080–2094. doi:10.1002/etc.5620211011

French-McCay, D. P., Jayko, K., Li, Z., Spaulding, M. L., Crowley, D., Mendelsohn, D., et al. (2021b). Oil Fate and Mass Balance for the Deepwater Horizon Oil Spill. *Mar. Pollut. Bull.* 171, 112681. doi:10.1016/j.marpolbul.2021.112681

French-McCay, D. P., Lehr, W., Stone, K., Fieldhouse, B., Dissanayake, A. L., Marcotte, G., et al. (2021a). "Floating Oil Emulsification – Review of Models, Input Requirements and Research Needs," in Proceedings of the 43rd AMOP Technical Seminar on Environmental Contamination and Response, June 8–10, 2021 (Ottawa, ON, Canada: Emergencies Science Division, Environment Canada).

French-McCay, D. P. (2004). Oil Spill Impact Modeling: Development and Validation. *Environ. Toxicol. Chem.* 23 (10), 2441–2456. doi:10.1897/03-382

French-McCay, D. (2016). "Potential Effects Thresholds for Oil Spill Risk Assessments," in Proceedings of the 39th AMOP Technical Seminar on Environmental Contamination and Response, Halifax, NS, June 7–9, 2016 (Environment Canada).39, 285–303.

French-McCay, D. P., Parkerton, T. F., and de Jourdan, B. (2022). Bridging the Lab to Field Divide: Advancing Oil Spill Biological Effects Models Requires Revisiting Aquatic Toxicology Testing. *Toxicology*. (in review).

IPIECA (2015). Response Strategy Development Using Net Environmental Benefit Analysis (NEBA). Report 527. London, UK: International Petroleum Industry Environmental Conservation Association IPIECA. Available at: http://www.ipieca.org/resources/good-practice/response-strategy- development-using-net-environmental-benefit-analysis-neba-good-practice-guidelines-for-incident- management-and-emergency-response-personnel/.

ITOPF (2018). *ITOPF Handbook*. London, United Kingdom: International Tanker Owners Pollution Federation, 55. Available at: http://www.itopf.com/knowledge-resources/documents-guides/document/itopf-handbook/.

Lehr, W. (2017). "Developing a New Emulsification Algorithm for Spill Response Models," in Proceedings of the Fortieth AMOP Technical Seminar on Environmental Contamination and Response, Calgary, AB, October 3–5, 2017 (Ottawa, ON: Environment Canada), 572–585.

Mackay, D., Buist, I., Mascarenhas, R., and Paterson, S. (1980a). Oil Spill Processes and Models. Report EE-8. Ottawa, Canada: Environmental Emergency Branch, Department of Fisheries and Environment, Environment Canada, 91p.

Mackay, D., Paterson, S., and Trudel, K. (1980b). *A Mathematical Model of Oil Spill Behavior*. Canada: Toronto, ON: Department of Chemical and Applied Chemistry, University of Toronto, 39p.

Mackay, D., Shiu, W. Y., Hossain, K., Stiver, W., McCurdy, D., and Peterson, S. (1982). Development and Calibration of an Oil Spill Behavior Model. Report No. CG-D-27-83. Groton, Connecticut: U.S. Coast Guard, Research and Development Center, 83p.

Mackay, D., and Zagorski, W. (1982). Water-In-Oil Emulsions. Manuscript Report EE-34. Ottawa, Ontario: Environment Canada, 93.

Mooney, M. (1951). The Viscosity of a Concentrated Suspension of Spherical Particles. *J. Colloid Sci.* 6, 162–170. doi:10.1016/0095-8522(51)90036-0

National Academies of Sciences, Engineering, and Medicine (NASEM) (2020). *The Use of Dispersants in Marine Oil Spill Response*. Washington, DC: The National Academies Press. doi:10.17226/25161

National Oceanic and Atmospheric Administration (NOAA) (2010). *Characteristics of Response Strategies: A Guide for Spill Response Planning in Marine Environments*. Seattle, WA: U.S. Department of Commerce, U.S. Coast Guard, U.S. Environmental Protection Agency, American Petroleum Institute, 75p.

National Oceanic and Atmospheric Administration (NOAA) (2016). *Open Water Oil Identification Job Aid for Aerial Observation*. Seattle, WA: U.S. Department of Commerce, Office of Response and Restoration. Available at: http://response.restoration.noaa.gov/oil-and-chemical-releases/oil-releases/resources/open-water-oil-identification-job-aid.html.

Payne, J. R., and McNabb, G. D., Jr. (1984). Weathering of Petroleum in the Marine Environment. *Mar. Technol. Soc. J.* 18 (3), 24–40.

Reed, M. (1989). The Physical Fates Component of the Natural Resource Damage Assessment Model System. *Oil Chem. Pollut.* 5, 99–123. doi:10.1016/s0269-8579(89)80009-7

Ward, C. P., Sharpless, C. M., Valentine, D. L., French-McCay, D. P., Aeppli, C., White, H. K., et al. (2018). Partial Photochemical Oxidation Was a Dominant Fate of Deepwater Horizon Surface Oil. *Environ. Sci. Technol.* 52 (4), 1797–1805. doi:10.1021/acs.est.7b05948

Zhao, L., Nedwed, T., Daling, P. S., and Brandvik, P. J. (2022). Investigation of the Spreading Tendency of Emulsified Oil Slicks on Open Systems. *Mar. Pollut. Bull.* (accepted).

Conflict of Interest: DF-M, MF, and MG were employed by RPS Oceans and Coastal, part of RPS Group, Inc.

Publisher's Note: All claims expressed in this article are solely those of the authors and do not necessarily represent those of their affiliated organizations, or those of the publisher, the editors and the reviewers. Any product that may be evaluated in this article, or claim that may be made by its manufacturer, is not guaranteed or endorsed by the publisher.